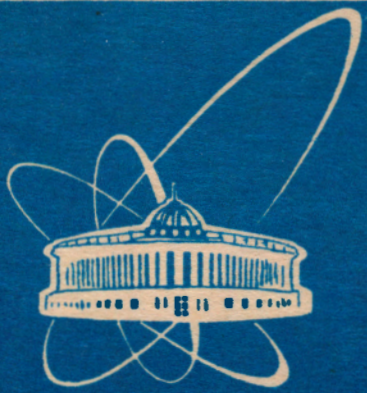

ОБЪЕДИНЕННЫЙ
ИНСТИТУТ
ЯДЕРНЫХ
ИССЛЕДОВАНИЙ

Дубна

E1-96-256

L.G.Afanasyev, O.E.Gorchakov, V.V.Karpukhin,
V.I.Komarov, V.V.Kruglov, A.V.Kulikov, A.V.Kuptsov,
L.L.Nemenov, M.V.Nikitin, Zh.P.Pustylnik, A.S.Chvyrov,
S.V.Trusov*, V.V.Yazkov*

MEASUREMENT OF THE COULOMB INTERACTION EFFECT IN $\pi^+\pi^-$ PAIRS FROM THE REACTION $p\mathrm{Ta} \to \pi^+\pi^- X$ AT 70 GeV

Submitted to «Ядерная физика»

*Institute for Nuclear Physics, Dubna Branch, Moscow State University, 141980 Dubna, Moscow Region, Russia

1996

1. Introduction

The differential production cross section for pairs of oppositely charged particles with a small relative momentum in the c.m.s. $q \sim 2\mu\alpha$ (μ is the reduced mass of the pair, α is the fine structure constant) may substantially increase owing to the Coulomb interaction of particles in the final state [1]. This effect takes place if the size of the production region $r_{\rm pr}$ is much smaller than the effective radius of the Coulomb interaction $r_C \sim 1/\mu\alpha =$ 387 fm:

$$r_{\rm pr} \ll r_C \tag{1}$$

Detected in inclusive processes $\pi^+\pi^-$ pairs can be separated into two types which are different with respect to the size of the $\pi^+\pi^-$ pair production region.

The $\pi^+\pi^-$ pairs of the first type are produced in direct processes and in decays of short-lived resonances (ρ, ω, Δ, ...). In this case a typical size of the pion production region is $r_{\rm pr} \sim 1 \div 20$ fm, much less than r_C. Pions in these pairs undergo the Coulomb interaction in the final state [2, 3] and they are called therefore "Coulomb" pairs.

The pion pairs of the second type are ones in which one or both particles come from long-lived sources (η, K^0_S, Λ, ...). A typical range between such pions at production is more than 10^3 fm and hence the Coulomb and strong interaction effects in the final state are negligible. These pairs are called hereinafter "non-Coulomb" pairs.

Therefore the differential cross section of $\pi^+\pi^-$ pair production can be written as:

$$\frac{d\sigma}{d\vec{p}_1\, d\vec{p}_2} = \frac{d\sigma_s}{d\vec{p}_1\, d\vec{p}_2} + \frac{d\sigma_l}{d\vec{p}_1\, d\vec{p}_2}, \tag{2}$$

where the indices s and l are the reminders of the short-lived and long-lived sources, respectively.

The production cross section of the "Coulomb" pairs can be written in the factorized form [1, 4] since the radii of the strong and Coulomb interactions are essentially different (1):

$$\frac{d\sigma_s}{d\vec{p}_1\, d\vec{p}_2} = A_c(q)\frac{d\sigma^0_s}{d\vec{p}_1\, d\vec{p}_2}, \tag{3}$$

where $d\sigma_s^0/d\vec{p}_1 d\vec{p}_2$ is the $\pi^+\pi^-$ pair production cross section without taking into account the Coulomb interaction in the final state and $A_c(q)$ is the Coulomb factor. For the nonrelativistic relative velocity of the particles $A_c(q)$ is written as [1]:

$$A_c(q) = -\frac{2\pi m\alpha/q}{\exp(-2\pi m\alpha/q) - 1}. \quad (4)$$

Here m is the particle mass. At small relative momenta ($q < 10$ MeV/c for $\pi^+\pi^-$ pairs) the Coulomb factor abruptly increases with decreasing q.

In the case of a relativistic velocity of $\pi^+\pi^-$ pairs relative to a residual nucleus the Coulomb interaction of the pions with the nucleus is insignificant [5].

The Coulomb interaction effect in the e^+e^- pair production was considered first by A.D. Sakharov [1]. Later the problem of the Coulomb interaction of charged particles in the final state was solved for arbitrary reactions with production of pairs having both small and relativistic relative momenta [6, 7]. The difference between the relativistic and nonrelativistic Coulomb factors for $q < 50$ MeV/c does not exceed 0.5%.

The Coulomb interaction must be taken into account in all processes where charged particles are produced. Let us give a few examples. The Coulomb interaction with nuclear fragments leads to distortion of the spectra of π^+ and π^- mesons produced in nucleus-nucleus collisions [8]. The Coulomb interaction of identical pions results in the reduction of a correlation function at small relative momenta [9]. The shape of the correlation function for production of two protons with small relative momentum is determined not only by Fermi statistics and nuclear forces but also by the Coulomb interaction [10]. The Coulomb interaction of charged pions from K meson decays increases the decay width of $K^\pm$ and K_L^0 mesons [11]. There are theoretical predictions for the value and consequence of the Coulomb interaction in the decay $\Upsilon(4s) \to B^+B^-$ [12] and for the W^+W^- pair production near the threshold [13].

A possibility of observing the Coulomb interaction effect in the differential production cross section for pairs of elementary particles was considered in paper [14]. For the first time the effect was observed in [15] where the yield of the $\pi^+\pi^-$ pairs with small relative momenta ($q < 40$ MeV/c) was measured in the pTa interaction at proton energy 70 GeV/c at the Serpukhov accelerator. A sharp increase in the $\pi^+\pi^-$ pair production was observed as relative momentum of pions decreased. The value of this effect

is consistent with the Coulomb factor. Later this effect was also observed in $\pi^+\pi^-$, $p\pi^-$ and K^+K^- pairs generated in pp collisions at 27.5 GeV/c [3].

In addition to production of oppositely charged particles in a free state the production of the Coulomb bound states (atoms) consisting of the same particles is possible. Production of $\pi^+\pi^-$ atoms $A_{2\pi}$ (and other hadronic atoms) in inclusive processes was considered in [14], where the method of observation of these atoms and their lifetime measurement were proposed too. The $\pi^+\pi^-$ atoms (dimesoatoms) are produced in inclusive processes in the S-states. The production cross section of $A_{2\pi}$ is proportional to a square of the atom wave function at the origin and to the double inclusive production cross section of π^+ and π^- mesons with small relative momenta. Consequently, the number of the atoms produced can be calculated from the number of free "Coulomb" pairs in some interval $q < q_0$. If q_0 is much less than the pion mass, then these two processes are practically indistinguishable in respect to the pair production dynamics.

The dimesoatom lifetime is inversely proportional to a square of the $A_{2\pi}$ wave function at the origin and to a difference squared $(a_0 - a_2)^2$ of the S-wave $\pi\pi$ scattering lengths with isospin 0 and 2 [16, 17]. In the chiral perturbation theory the a_0 and a_2 were calculated with the precision of 5% [18] and the predicted $A_{2\pi}$ lifetime in the 1S-state equals $\tau = (3.7 \pm 0.3) \cdot 10^{-15}$ s. Thus the precise measurement of the dimesoatom lifetime is of crucial importance for the test of the chiral theory.

The lifetime of $A_{2\pi}$ is very small. Thus the atoms produced in inclusive processes can be observed, essentially, only through the detection of the $\pi^+\pi^-$ pairs ("atomic" pairs) from the $A_{2\pi}$ breakup in the same target where they are produced [14]. Most of the "atomic" pairs (95%) have the relative momentum $q < 3$ MeV/c. Thus the "atomic" pairs are located in the region of the Coulomb enhancement.

The number of the $\pi^+\pi^-$ pairs from the $A_{2\pi}$ breakup depends on the relation between the probabilities of the annihilation $\pi^+\pi^- \to \pi^0\pi^0$ and of the breakup in the material of the target. If the breakup probability is known (it can be calculated within 1% [19]) the dimesoatom lifetime can be determined using the ratio of the number of the "atomic" pairs detected to the number of the atoms produced.

The "atomic" $\pi^+\pi^-$ pairs were first observed [20] in the pTa interaction at proton energy 70 GeV/c with the same experimental setup that was used for observation of the Coulomb effect [15]. The first experimental estimation of the $A_{2\pi}$ lifetime was also obtained [21].

In connection with the proposed experiment on the $A_{2\pi}$ lifetime measurement with the precision of 10% [22] a detailed analysis of the statistical data used for the dimesoatom observation [20] and the $A_{2\pi}$ lifetime estimation [21] is carried out with a goal to estimate the precision of the Coulomb peak description by different approximating functions. A possibility of separating pairs of charged particles with respect to the size of their production region have also been investigated.

2. Experimental setup

The experimental setup (Fig. 1) for the study of the Coulomb effect and $\pi^+\pi^-$ atoms was described in Refs. [15, 20]. The $\pi^+\pi^-$ pairs were produced in a tantalum target of 8 μm ("thick" target) or 1.4 μm ("thin" target) thick inserted into the internal proton beam of the accelerator, then got into a 40 m long vacuum channel (the acceptance is $3.8 \cdot 10^{-5}$ sr) placed at 8.4° to the proton beam and were finally detected by a magnetic two-arm spectrometer in the $0.8 \div 2.4$ GeV/c pion momentum interval.

The channel was connected to the accelerator vacuum pipe without any partition and was shielded against the accelerator's and Earth's magnetic fields. The channel was terminated with a flat vacuum chamber located between the spectrometer magnet poles ($B = 0.85$ T).

Charged particles were detected by telescopes T_1 and T_2. The track coordinates were measured by drift chambers (DC). The time interval between detector hits in T_1 and T_2 was measured by scintillation hodoscopes (H_1, H_2). Electrons and positrons were rejected by gas Cherenkov counters ($\check{C}_1$, $\check{C}_2$), and muons by scintillation counters (S_{μ_1}, S_{μ_2}) placed behind cast-iron absorbers. Besides π mesons other charged hadrons were detected. A rate of proton-target interaction was monitored with γ-flux measurements and amounted to about $7 \cdot 10^8$ per 0.7 s spill. The detector counting rate was about 10^5 per spill.

The first-level trigger was formed by the coincidence signals from the telescopes $(H_1 S_1 \overline{C}_1 \overline{S}_{\mu_1}) \times (H_2 S_2 \overline{C}_2 \overline{S}_{\mu_2})$ (Fig. 1). The second-level trigger was generated by a special processor which selected tracks having small angles to the channel axis in a vertical plane (less than $3.3 \cdot 10^{-2}$ rad) and a vertical coordinate difference $|Y_1 - Y_2|$ in T_1 and T_2 less than 80 mm. The number of events per spill written on magnetic tapes was about 90. The total statistics collected with the "thick" and "thin" targets contains $1.3 \cdot 10^7$ events.

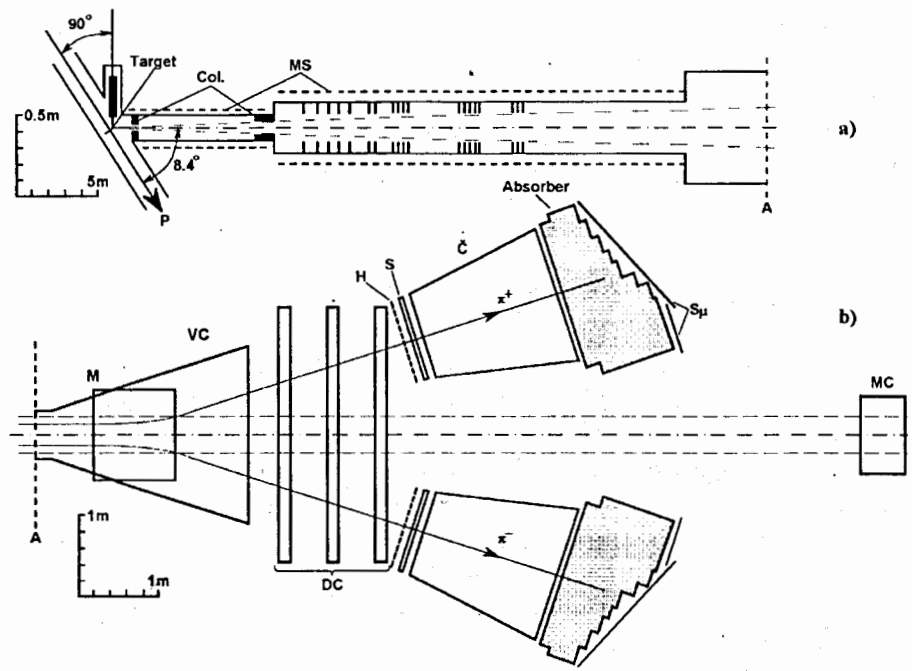

Figure 1: Experimental setup: a) — channel scheme: p — internal proton beam, Target — target mechanism, Col — collimators, MS — magnetic shield; b) — magnet and detectors: M — poles of spectrometer magnet, VC — vacuum chamber, DC — drift chambers, H — scintillation hodoscopes, S, S_μ — scintillation counters, Č — gas Cherenkov counters, Absorber — cast-iron absorber, MC — monitor counters.

The measurements and simulation allowed us to obtain the setup resolution for the pion momentum $\sigma_p/p = 0.008$, for the deviation of the track projections from direction towards the target in the vertical plane $\sigma_{\phi_1} = \sigma_{\phi_2} = 1.2$ mrad and for the opening angle of pairs upstream of the magnet $\sigma_{\theta_{1,2}} = 0.1$ mrad. The resolution for the projections of $\pi^+\pi^-$ pair relative momentum in c.m.s. $\vec{q}$ onto the direction of the mean momentum $\vec{p} = (\vec{p}_1 + \vec{p}_2)/2$ of pions in a pair (q_L) and onto the plane XY perpendicular to $\vec{p}$ ($q_T^2 = q_X^2 + q_Y^2$) were $\sigma_{q_L} = 1.3$ MeV/c, $\sigma_{q_X} = \sigma_{q_Y} = 0.60$ MeV/c for the "thick" target and $\sigma_{q_L} = 1.3$ MeV/c, $\sigma_{q_X} = \sigma_{q_Y} = 0.44$ MeV/c for the "thin" target. The above resolutions are averaged over the pion momentum interval $0.8 \div 2.4$ GeV/c.

3. Data processing

At the data processing the space reconstruction of events was performed. The events recorded on the DST met the following requirements: presence of only a single track in the drift chambers of each telescope and the track passage through the hit counter of the scintillation hodoscope. The parameters of the tracks were corrected for the residual magnetic field in the channel and for the horizontal component of the spectrometer magnet field. The particle momenta and the track coordinates at the magnet entrance were calculated under the assumption that the particles came from the target.

The angles ϕ_{y_1} and ϕ_{y_2} in T_1 and T_2 between the track projections and the direction towards the target in the vertical plane were also determined. The FWHM of the ϕ_{y_1} and ϕ_{y_2} distributions for particles coming from the target equals $2.5 \cdot 10^{-3}$ rad (Fig. 2) and it is in accordance with the simulation. Pairs originating in the target were selected by applying the cut $\phi_y \leq 3.5 \cdot 10^{-3}$ rad, where $\phi_y = (\phi_{y_1}^2 + \phi_{y_2}^2)^{\frac{1}{2}}$, and by some other geometrical criteria.

To obtain the difference of the particle production times $t_{\rm pr} = t_1 - t_2$ (Fig. 3) the time difference between the particle hits in the hodoscopes was corrected for the time of flight of particles from the target to the hodoscope (particle mass was assumed equal to π meson mass), for the time of light transmission in the scintillators and for the delay spread in the channels of the hodoscopes. The distribution contains the true coincidence peak ($\sigma = 0.8$ ns) and the uniform background of accidental coincidences. The interval $\Delta t_2 = 2.56$ ns was used to obtain the sum N_{ta} of true and

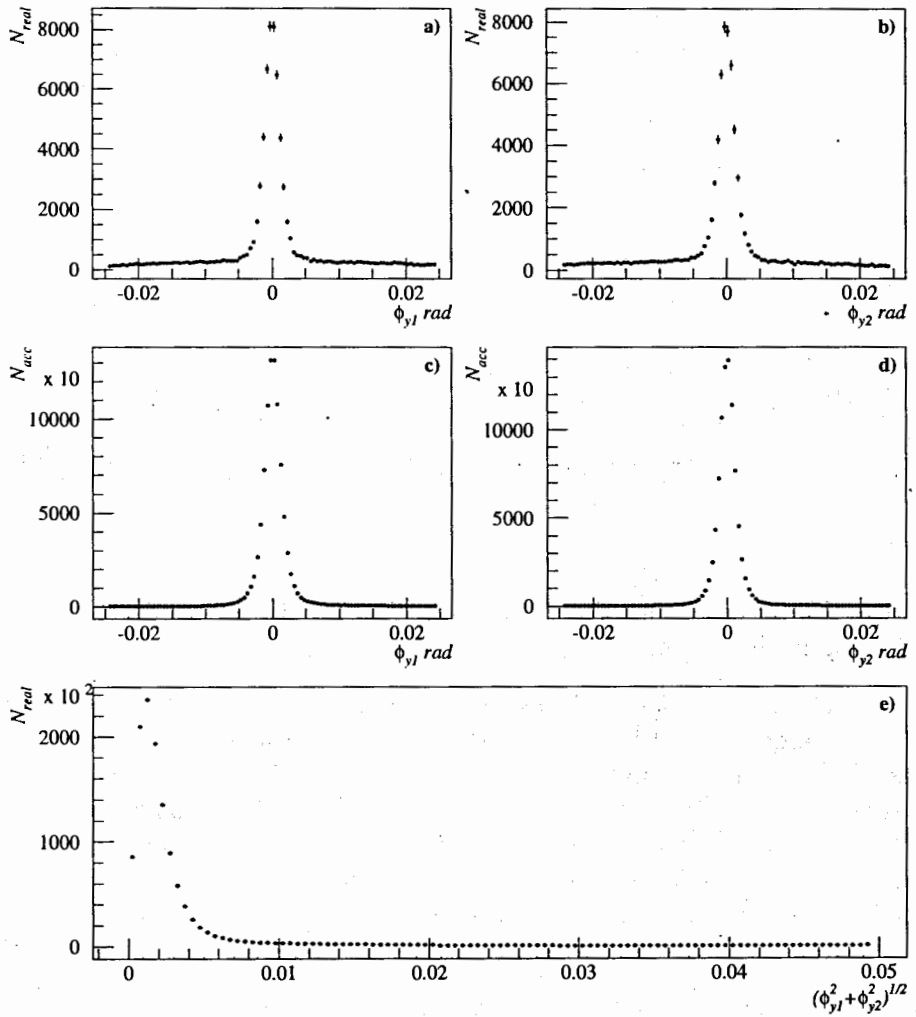

Figure 2: Distribution of particles from real ($N_{\rm real}$) and accidental ($N_{\rm acc}$) pairs over the angles $\phi_{y_{1,2}}$ between the track projections and the direction towards the target in the vertical plane in the spectrometer arm T_1 (a, c) and T_2 (b, d). The number of detected events versus $(\phi_{y_1}^2 + \phi_{y_2}^2)^{\frac{1}{2}}$ is shown in the lower axes.

accidental events, and the intervals $\Delta t_1 = \Delta t_3 = 8.0$ ns to determine the number of accidental events N_a under the true coincidence peak in Δt_2. In the interval Δt_2 the ratio of true to accidental events equals 0.36.

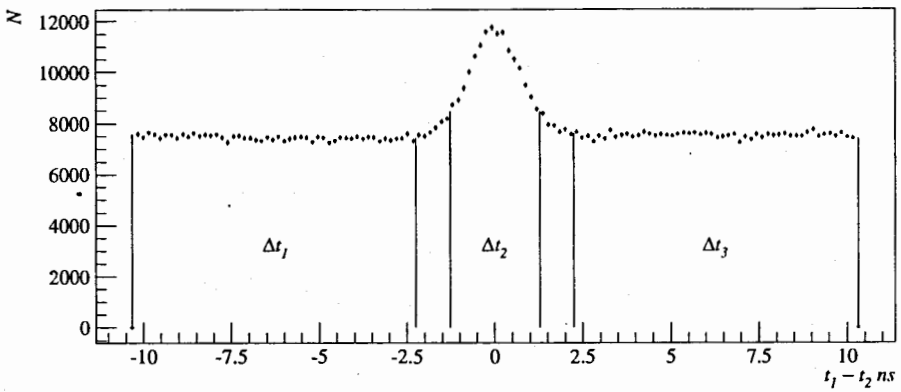

Figure 3: Distribution over the measured time difference of particle production in the target.

The true coincidences N_t are caused mainly by $\pi^+\pi^-$ pairs produced in the target. The fraction of background $\pi^+\pi^-$ pairs generated in the accelerator vacuum pipe and in the beryllium target holder was measured to be less than 3% of N_t. The measurements and simulation have shown that $\pi^+\pi^-$ pairs from K^+, K^- and K^0_L decays are strongly reduced by cut on ϕ_y and their amount is about $10^{-2}\,N_t$. The admixtures of K^+K^- and $p\bar{p}$ pairs are equal to $10^{-4}\,N_t$ and $5 \cdot 10^{-3}\,N_t$, respectively. The e^+e^- pair admixture due to some inefficiency ($\sim$1%) of the Cherenkov counters is $6 \cdot 10^{-3}\,N_t$. The π^+K^-, π^-K^+, $\pi^+\bar{p}$ and π^-p pairs are absent in the true coincidence peak because times of flight of π, K and p from the target to the hodoscopes are substantially different. From above it follows that the $\pi^+\pi^-$ pairs constitute more than 97% of the total number of true events detected.

The true event distribution over q (and on other variables) was found from the obvious relation:

$$\frac{dN_t}{dq} = \frac{dN_{ta}}{dq} - \left[\frac{\Delta t_2}{\Delta t_1 + \Delta t_3}\right] \frac{dN_a}{dq} \,. \qquad (5)$$

An example of the real and accidental pair distributions over q_L and modelled function are shown in Fig. 4.

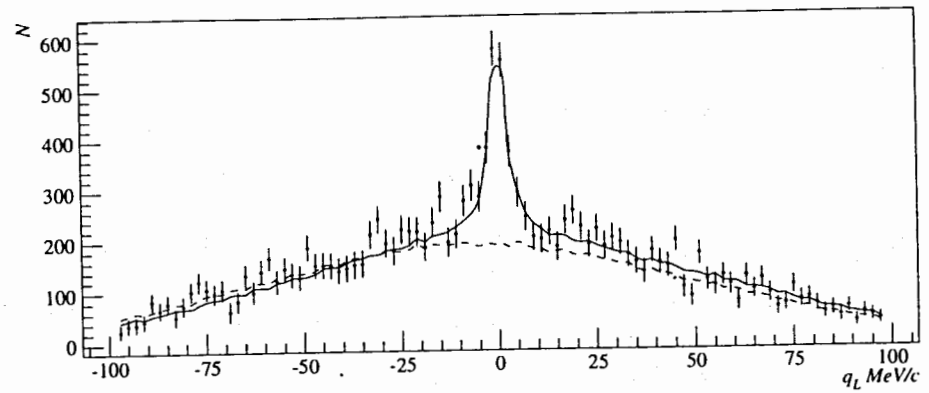

Figure 4: Distribution of real $\pi^+\pi^-$ pairs over q_L. Solid line is the modelled function, dashed line is the distribution of accidental pairs

Overall range of the relative momentum q was separated into two intervals. In the first interval ($q < 3$ MeV/c) the true coincidence distribution contains "atomic" and "free" pairs. The "free" pairs include both "Coulomb" and "non-Coulomb" pairs. In the second one ($q > 3$ MeV/c) this distribution contains only "free" pairs.

For fitting the experimental distribution over q the region $q > 3$ MeV/c was used. The interval $q < 3$ MeV/c is very interesting for study because at $q \to 0$ the Coulomb factor abruptly increases. However, the presence of the "atomic" pairs does not allow doing it in an explicit form.

A number of "atomic" pairs was determined in the range $q < 2$ MeV/c, where the best effect-to-error ratio is achieved. The total number of true events N_t at $q < 2$ MeV/c consists of the "atomic" N_A, "Coulomb" N_C and "non-Coulomb" N_n pairs:

$$N_t = N_A + N_C + N_n \,. \qquad (6)$$

The distribution dN_t/dq was fitted at $q > 3$ MeV/c with an approximating function (see below). Then the number of "Coulomb" N^f_C and

"non-Coulomb" N_n^f pairs in the region $q < 2$ MeV/c was determined using the parameters obtained by the fit.

The experimental number of the "atomic" pairs N_A was found from the relation:

$$N_A = N_t - (N_C^f + N_n^f) \,. \tag{7}$$

The number of the expected "atomic" pairs N_A^f relates uniquely to N_C^f:

$$N_A^f = N_C^f C P_{\rm br} P_q \,, \tag{8}$$

where C — the exactly calculated coefficient connecting the number of the $A_{2\pi}$ produced to the number of the "Coulomb" pairs in the interval $q < 2$ MeV/c — is determined by relation (12) in ref. [14] in view of the experimental condition; $P_{\rm br}$ — the probability of the $A_{2\pi}$ breakup in the target — is calculated using the breakup and discrete transition cross sections [19] taking into account the quantum number distribution of the dimesoatoms produced; P_q is part of the "atomic" pairs at $q \le 2$ MeV/c.

The difference between the experimental N_A and expected N_A^f numbers of the "atomic" pairs

$$N_A - N_A^f = N_t - (N_C^f + N_C^f C P_{\rm br} P_q + N_n^f) \tag{9}$$

is mainly determined by a precision of the "Coulomb" pair number predicted at $q < 2$ MeV/c from description of the q-distribution of N_t at $q > 3$ MeV/c.

Here we present the values C and $P_{\rm br}$ as calculated for the experimental conditions [20] for the "thick" (tk) and "thin" (tn) targets:

$$C^{\rm tk} = 0.73, \quad C^{\rm tn} = 0.69 \,. \tag{10}$$

$$P_{\rm br}^{\rm tk} = 0.414, \quad P_{\rm br}^{\rm tn} = 0.102 \,. \tag{11}$$

$$P_q^{\rm tk} = 0.78, \quad P_q^{\rm tn} = 0.83 \,. \tag{12}$$

The difference between the coefficients C for the "thick" and "thin" targets is due to different multiple scattering in the "thick" and "thin" targets. In the calculation of $P_{\rm br}$ the $A_{2\pi}$ the lifetime in the ground state was taken to be equal to $3.7 \cdot 10^{-15}$ s. The accuracy of the coefficients C is about 1% and for $P_{\rm br}$ it is about several percent.

4. Procedure of the Coulomb peak description

In the construction of the approximating function the distribution of the accidental coincidences of π^+ and π^- mesons is taken as a basis. The thing is that the distribution of these pairs $W(\vec{p}_1, \vec{p}_2)$ and the double inclusive cross section of the pion production $d\sigma/d\vec{p}_1 d\vec{p}_2$ are both proportional to the product of the single particle differential cross sections:

$$W(\vec{p}_1, \vec{p}_2) \sim \frac{d\sigma}{d\vec{p}_1} \frac{d\sigma}{d\vec{p}_2} \tag{13}$$

$$\frac{d\sigma}{d\vec{p}_1\, d\vec{p}_2} = \frac{1}{\sigma_{in}} \frac{d\sigma}{d\vec{p}_1} \frac{d\sigma}{d\vec{p}_2} R_{\rm pr}(s, A, \vec{p}, \vec{q}) \,, \tag{14}$$

where $d\sigma/d\vec{p}_1$ and $d\sigma/d\vec{p}_2$ are the single- particle inclusive cross sections, σ_{in} is the inelastic cross section, $R_{\rm pr} = A_c(q)\, R_s$ is a correlation function that incorporates Coulomb ($A_c(q)$) and strong (R_s) interactions, s is the total energy squared in c.m.s., A is the mass number of the target nucleus.

Comparison of Eqs.(13) and (14) shows that the difference in the true and accidental pair distributions is caused by the interaction in the final state alone. The efficiency of the detection of the true and accidental pairs is the same and it is determined only by the momenta of the particles. This allows the distribution of pairs from the accidental coincidences of π mesons $\Phi(q)$ ("phase space") to be used for description of the true pair distribution.

The distribution $\Phi(q)$ was obtained from the accidental event distribution dN_a/dq by introducing the weight $W_{\pi\pi} = W_1(p_1) \cdot W_2(p_2)$. Here $W_1(p_1)$ ($W_2(p_2)$) is a probability that the positively (negatively) charged particle is the π^+ (π^-) meson (see Fig. 5c and 5d). The fraction of protons in the momentum interval $0.8 \div 2.4$ GeV/c was calculated to be $N_{\rm p}/N_{\pi^+} = 0.65$. This ratio was measured in this experiment for the interval $0.8 \div 1.4$ GeV/c and it coincides with the Lund model calculation within 5%. The ratio of K mesons to pions is below 0.3%.

In Fig. 5a and 5b the π^+ and π^- lab momentum distributions from the true and accidental coincidences obtained with the functions $W_1(p_1)$ and $W_2(p_2)$ are shown. The distributions of π^- mesons practically fit each other ($\chi^2/n = 40/55$). For π^+ mesons the agreement is somewhat worse ($\chi^2/n = 127/55$) but the shape of the momentum distribution only indirectly affects

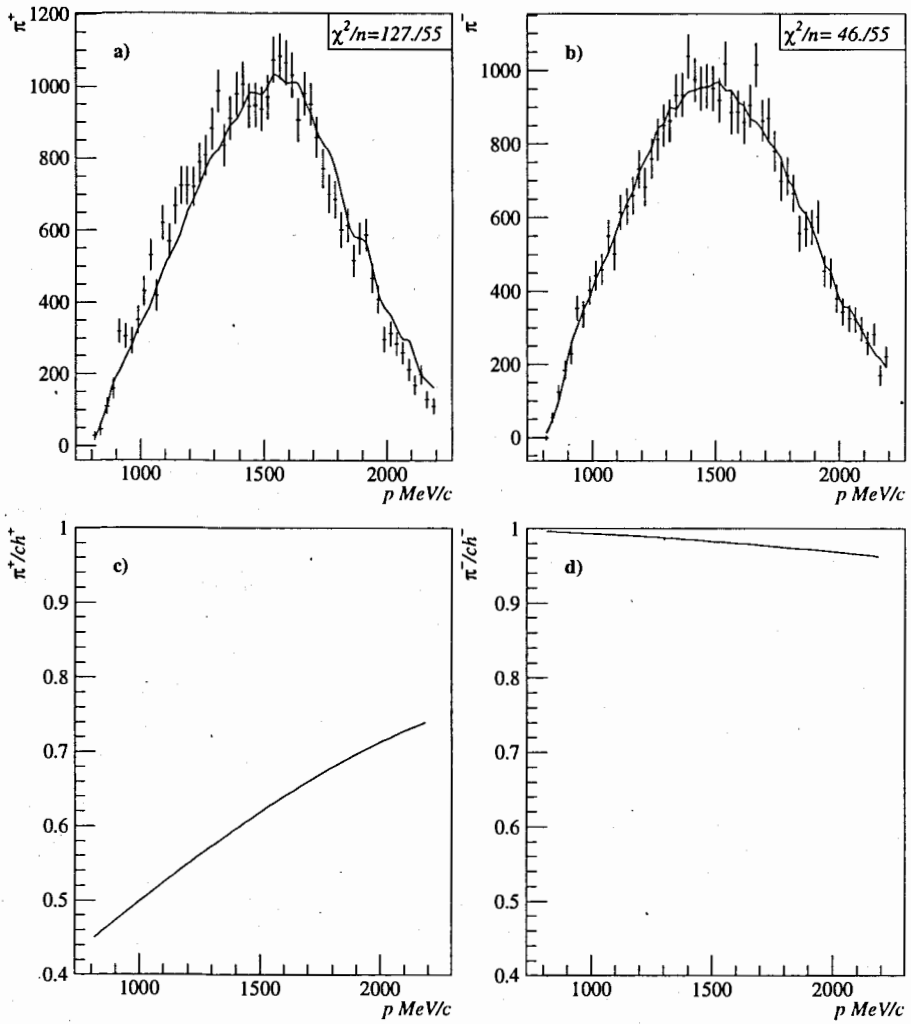

Figure 5: Spectra of π mesons from real (bars) and accidental (solid curve) pairs: a) positive particles, b) negative particles. Spectra for accidental pairs was obtained taking into account the ratio of π^+ mesons to all positively charged particles (c) and the same ratio for negative ones (d). These ratios are calculated with FRITIOF 6.0.

the relative momentum distribution of the pairs. Thus at the present level of precision this consistency suffices. That was substantiated by additional treatment of the data, its results being brought below.

The distribution $\Phi(q)$ is the sum of the pair distributions $\Phi(q)w_s(q)$ from short-lived sources and $\Phi(q)[1-w_s(q)]$ from long-lived sources. Here the weight $w_s(q)$ is the probability that both pions in an accidental pair originate from short-lived sources.

The distribution $\Phi(q)w_s(q)$ corresponding to "Coulomb" pairs should be multiplied by the Coulomb factor but this cannot be done directly. Because of multiple scattering of π mesons in the target and the finite resolution of the detectors, the relative momentum q measured by the setup differs from the momentum $q_{\rm real}$ that pairs have after production, which determines the value of the Coulomb interaction in the final state and, consequently, the value of $A_c(q)$.

For adequate description of the Coulomb interaction the following procedure was realized. For each detected accidental pair the momenta $\vec{p}_1$, $\vec{p}_2$ and the corresponding relative momentum q were determined. Then the pair production point inside the target depth, multiple scattering of π mesons in the target material and in the setup constituents and the errors in $\vec{p}_1$ and $\vec{p}_2$ reconstruction were simulated with Monte-Carlo method. As a result, the values of $\vec{p}_1\,'$, $\vec{p}_2\,'$ and q' were obtained. The distribution over the difference $q-q'$ corresponds to the distribution over the difference of the measured and true relative momenta of the pairs $q-q_{\rm real}$. Calculating the Coulomb weight $A_c(q)$ for q' and ascribing it to the pair with the momenta $\vec{p}_1$, $\vec{p}_2$ and q we obtain the distribution $K(q)=A_c(q')\Phi(q)$ of the pairs with the experimentally measured parameters of particles and modified Coulomb factor $A_c(q')$ like it occurs in the case of the true coincidences of $\pi^+\pi^-$ mesons from short-lived sources.

Using the distributions $\Phi(q)$ and $K(q)$ we can write a function $G(q)$ describing the experimental distribution of the true $\pi^+\pi^-$ pairs:

$$G(q)=n\left\{(1-z\,q)w_s(q)K(q)+[1-w_s(q)]\Phi(q)\right\}\ , \qquad (15)$$

where n is the normalization factor. The factor $(1-z\,q)$ accounts for the strong interaction in the final state, its form will be justified below.

We are interested in the q dependences of $w_s(q)$ and $(1-z\,q)$ only in the interval $0<q<50$ MeV/c only.

In general, the probability that both pions in an accidental pair originate from short-lived sources is the function $W_s(p,q)$ of the mean and

relative momenta of a pair. The function $w_s(q)$ can be written as:

$$w_s(q) = \frac{\int_{p_m-\Delta p/2}^{p_m+\Delta p/2} \frac{dN_t}{dp\,dq}\varepsilon(p,q)W_s(p,q)dp}{\int_{p_m-\Delta p/2}^{p_m+\Delta p/2} \frac{dN_t}{dp\,dq}\varepsilon(p,q)dp} \qquad (16)$$

where p_m is the middle and Δp is the width of the mean momentum interval of the data sample used. The simulation has shown that under experimental conditions ($q < 50$ MeV/c and $800 < p < 2200$ MeV/c) W_s does not depend on q: $W_s = W_s(p)$. Also, the distribution of pions can be factorized $dN_t/dp\,dq \sim F(p)H(q)$ and its dependence on q in w_s is canceled. However the $\pi^+\pi^-$ pair detection efficiency as a function of q varies with p, i.e. $\varepsilon(p,q) \neq \varepsilon(p)\varepsilon(q)$ and this fact leads to the dependence of w_s on q. This dependence can be diminished by dividing the statistical data into narrow intervals Δp. To exclude it totally, the events should be selected in such a way that the q-dependence of the detection efficiency will be the same for all values of p, i.e. the detection efficiency should be a factorized function of p and q: $\varepsilon(p,q) = \varepsilon(p)\varepsilon(q)$.

The strong correlation function R_s can be factorized in the form [23]:

$$R_s(q) = (1 + F(q))\,S(q^2)\,, \qquad (17)$$

where $F(q)$ and $S(q^2)$ include the $\pi\pi$ interaction in the final state and the dynamics of $\pi^+\pi^-$ pair production, respectively.

The relative change of $S(q^2)$ in the range of q from 0 to 50 MeV/c is about $4\cdot10^{-3}$ [23]. This result is explained by the small difference of $\pi^+\pi^-$ effective mass $M_{\pi\pi}$ from $2m_\pi$: $M_{\pi\pi} = 2m_\pi + 4.4$ MeV at $q = 50$ MeV/c.

The correlation function $F(q)$ was obtained in the framework of the independent source model [10, 24, 25]. In the interval $0 \le q \le 30$ MeV/c it can be written as a linear function:

$$F(q) = F_0 - \xi q\,. \qquad (18)$$

It was found that the coefficient ξ does not depend on the model parameters and equals $\xi \approx 1.2\cdot10^{-3}$ (MeV/c)$^{-1}$. It should be pointed out that F_0 depends on p.

The hadron correlation function $R_s(q)$ varies only by ~6% in the interval $0 \le q \le 50$ MeV/c. This is confirmed by the experimental observation [20]. Thus for taking into account the effects of the strong interaction in the final state the linear function $(1 - z\,q)$ written in (15) is sufficient.

Practically, the experimental distribution of the true pairs was fitted by the functions of two kinds that were obtained on the basis of $\Phi(q)$. The first one was constructed on the assumption that $w_s(q) = const$ and had two free parameters n and w

$$G(q) = n\big[wK(q) + (1-w)\Phi(q)\big]\,. \qquad (19)$$

The hadron correlation function was not taken into account in this case.

The other function was used for a joint fit of the q-distributions in a few intervals of the mean momentum p. This allows for the dependence $w_s(q)$. In the ith interval the function is determined by three parameters w_i ($i = 1, 2, \ldots$) and n and a which were common for all intervals:

$$G(q) = n\big[(1 - a\,p_i^m)w_iK(q) + (1-w_i)\Phi(q)\big]\,. \qquad (20)$$

The parameter a takes into account the variation of amount of the pairs from short-lived sources through dependence of the hadron correlation function on the lab momentum at $q = 0$ (18). The p_i^m is the middle momentum of π mesons in the ith interval. The factor which describes the dependence of the hadron correlation on q (15) is not included because the analysis has shown that the coefficient z is not statistically significant.

5. Results

The pairs with the mean momentum in the interval $800<p<2200$ MeV/c divided into 8 parts of 175 MeV/c width were selected for analysis. The relative-momentum distribution of true coincidence pairs (the experimental distribution) was fitted by the two-parameter modelled function $G(q)$ (19) in each part and in the intervals consisting of two or four parts and in the whole region.

Figures 6a–6c show the event distributions over q and its projections q_L and q_T for the mean momenta $1500 < p < 1850$ MeV/c obtained on the "thick" target. The pairs with $q > 3$ MeV/c were sampled to exclude the "atomic" pairs. The fall in the distribution over q_L near zero is explained by this cut.

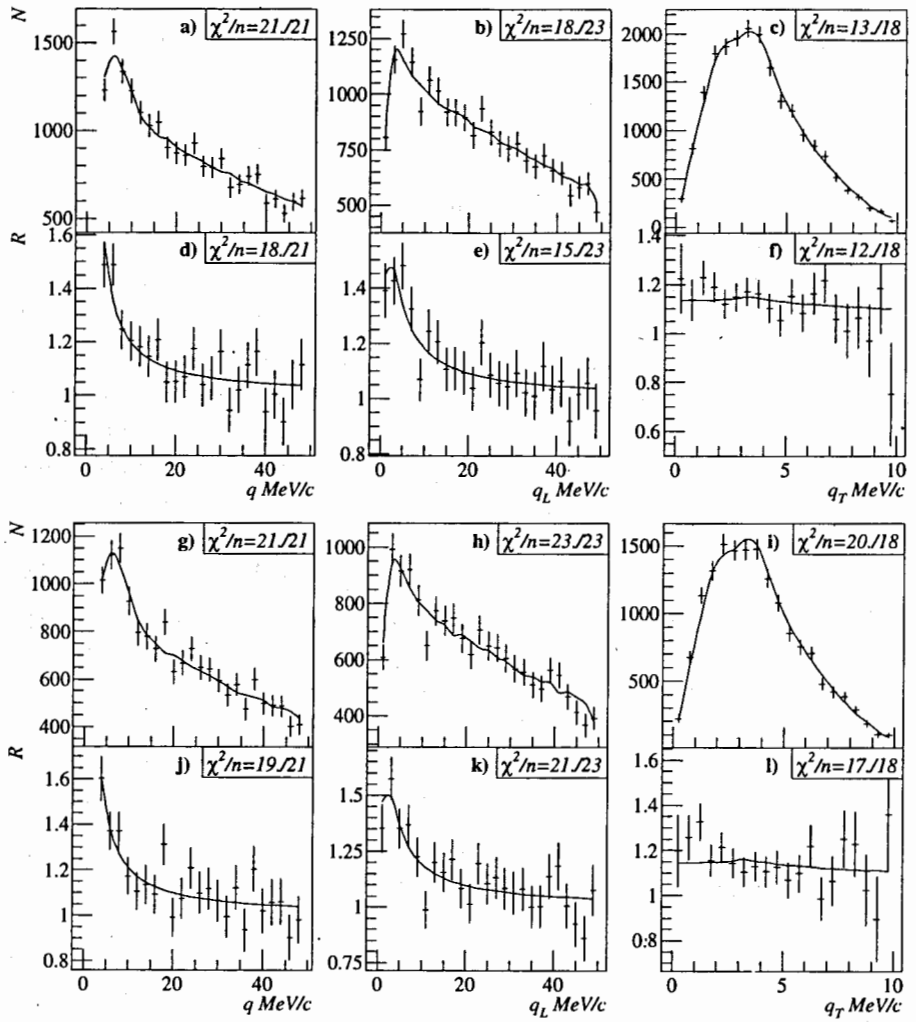

Figure 6: The event distributions over the relative momentum q in the interval $3 < q < 50$ MeV/c obtained with the "thick" target (a) and over its projections q_L (b) and q_T (c) for the same data. The mean momentum range is $1500 < p < 1850$ MeV/c. Solid lines are modelled functions. Distributions (d), (e) and (f) show the same data presented in the form of correlation functions. Distributions (g–l) obtained with the "thin" target are analogous to (a–f) ones.

In Figs. 6d–6f the same data are presented in the form of the correlation function:

$$R(q) = \frac{1}{n}\frac{N(q)}{\Phi(q)}. \qquad (21)$$

Here $N(q)$ is the experimental distribution, $\Phi(q)$ is the "phase space", n is a normalization coefficient of the modelled function $G(q)$ (19). This normalization provides $R \to 1$ at $q \to \infty$. For the correlation function determined in this way the detection efficiency and the setup acceptance are excluded.

In Figs. 6g–6i the event distributions analogous to those in Fig. 6a–6c obtained with the "thin" target are presented. In Figs. 6j–6l the corresponding correlation functions are shown.

It is seen that the value of the correlation function increases with decreasing relative momentum from 1.1 at $q = 15$ MeV/c to 1.6 at $q = 3$ MeV/c (Fig. 6j). The distribution over q_T does not contain the "Coulomb" peak at small q_T because it is integrated over q_L and hence for different q_T the average values of q, which determine the "Coulomb" factor, are similar.

In all the figures one also sees the modelled curves whose parameters were obtained by fitting only the q-distributions. Good description of the distributions over the q projections confirms the correctness of the procedure used.

For estimation of the description quality of the event distributions it is appropriate to use χ^2 values for the correlation functions because the modelled function $G(q)$ based on the distribution of accidental pairs contains statistical errors as well. These errors do not take into accounted the statistical errors of the experimental distribution and the χ^2 values become larger. The correlation function is free of this shortcoming because the errors of both the true pair distribution and "phase space" are included in the errors of $R(q)$.

The χ^2 values and fit parameters w and n for different intervals of the mean momentum $[p_{\min}, p_{\max}]$ for the two target thicknesses are listed in Table 1. Rather bad χ^2 values in the first and last intervals are explained by strong dependence of the range (q_L, q_T) for the detected pairs on the pion mean momentum near the boundary of the spectrometer acceptance and, consequently, by higher sensitivity of the fit procedure to the variation of the ratio between the "Coulomb" and "non-Coulomb" pairs in these momentum intervals.

Table 1:

p_{min} MeV/c	p_{max} MeV/c	thick target		
		χ^2/n	w	n
800.	1150.	33/21	0.66 ± 0.14	0.1013 ± 0.0043
1150.	1500.	26/21	0.455 ± 0.075	0.1012 ± 0.0022
1500.	1850.	18/21	0.552 ± 0.079	0.0861 ± 0.0020
1850.	2200.	31/21	0.57 ± 0.17	0.0812 ± 0.0041
		thin target		
800.	1150.	25/21	0.51 ± 0.15	0.1062 ± 0.0051
1150.	1500.	13/21	0.619 ± 0.096	0.0986 ± 0.0026
1500.	1850.	19/21	0.588 ± 0.089	0.0922 ± 0.0023
1850.	2200.	19/21	0.70 ± 0.19	0.0849 ± 0.0047

The data in Table 1 show that the normalization coefficient n depends on the mean momentum p. Probably, it is explained by the momentum dependence of the hadron correlation function (18) at $q = 0$. The values of w_s are practically the same for the different momentum intervals taking into account the errors.

The experimental numbers of the "atomic" pairs N_A obtained for the "thick" and "thin" targets by data fitting in eight, four, two intervals and in the whole momentum range are listed in Table 2. In addition, there are also the values of N_A^s obtained by summing N_A in the intervals of the mean momentum of 175 MeV/c wide presented in the first eight lines of Table 2.

Comparison of N_A and N_A^s in the momentum intervals of different width shows that for the widths up to 700 MeV/c the difference is practically absent. Only in the whole momentum region N_A increases as compared with N_A^s. This difference cannot be due to statistical fluctuation because the values of N_A and N_A^s are based on the same data sample. It is explained by dependence of the $w_s(q)$ behavior on the momentum interval width. Consequently, for the given statistics the dependence of the ratio of the short-lived to long-lived sources on the momentum p, which is responsible for $w_s = w_s(q)$ does not influence the results for the interval width which is less than or equals to 700 MeV/c.

To obtain the sensitivity of the description of the experimental data to the modelled function we performed an additional fit with four different functions:

Table 2:

p_{min} MeV/c	p_{max} MeV/c	thick target		thin target	
		N_A	N_A^s	N_A	N_A^s
800.	975.	-1. $\pm$ 24.		1. $\pm$ 20.	
975.	1150.	39. $\pm$ 32.		-2. $\pm$ 28.	
1150.	1325.	121. $\pm$ 32.		14. $\pm$ 30.	
1325.	1500.	101. $\pm$ 32.		3. $\pm$ 27.	
1500.	1675.	-8. $\pm$ 31.		17. $\pm$ 27.	
1675.	1850.	102. $\pm$ 26.		31. $\pm$ 21.	
1850.	2025.	5. $\pm$ 16.		-5. $\pm$ 13.	
2025.	2200.	5. $\pm$ 4.		-3. $\pm$ 4.	
800.	1150.	30. $\pm$ 39.	39. $\pm$ 40.	1. $\pm$ 34.	-1. $\pm$ 34.
1150.	1500.	224. $\pm$ 45.	222. $\pm$ 46.	14. $\pm$ 40.	16. $\pm$ 41.
1500.	1850.	99. $\pm$ 40.	94. $\pm$ 40.	48. $\pm$ 34.	47. $\pm$ 34.
1850.	2200.	13. $\pm$ 16.	10. $\pm$ 17.	-7. $\pm$ 14.	-8. $\pm$ 14.
800.	1500.	264. $\pm$ 59.	261. $\pm$ 60.	11. $\pm$ 52.	15. $\pm$ 53.
1500.	2200.	116. $\pm$ 43.	104. $\pm$ 44.	44. $\pm$ 37.	39. $\pm$ 37.
800.	2200.	404. $\pm$ 72.	365. $\pm$ 74.	71. $\pm$ 62.	55. $\pm$ 65.

1. Modelled distribution of the "Coulomb" pairs $K(q)$ only.

2. Sum of the distributions of the "Coulomb" $K(q)$ and "non-Coulomb" $\Phi(q)$ pairs at their ratio calculated with the Lund model.

3. Sum of the distributions of the "Coulomb" and"non-Coulomb" pairs (19). Their ratio was determined independently by fitting the experimental distributions in the eight momentum intervals. In order to obtain the correlation function for the total momentum range the values of the modelled correlation functions of all intervals were averaged taking into account statistical errors.

4. Three-parameter function (20). The fit was accomplished jointly in the eight intervals with the subsequent averaging.

The results are shown in Figs. 7a–7d and in Figs. 7e–7h for the "thick" and "thin" targets, respectively. As is seen from Fig. 7, the best agreement with the experiment is achieved with the three-parameter function.

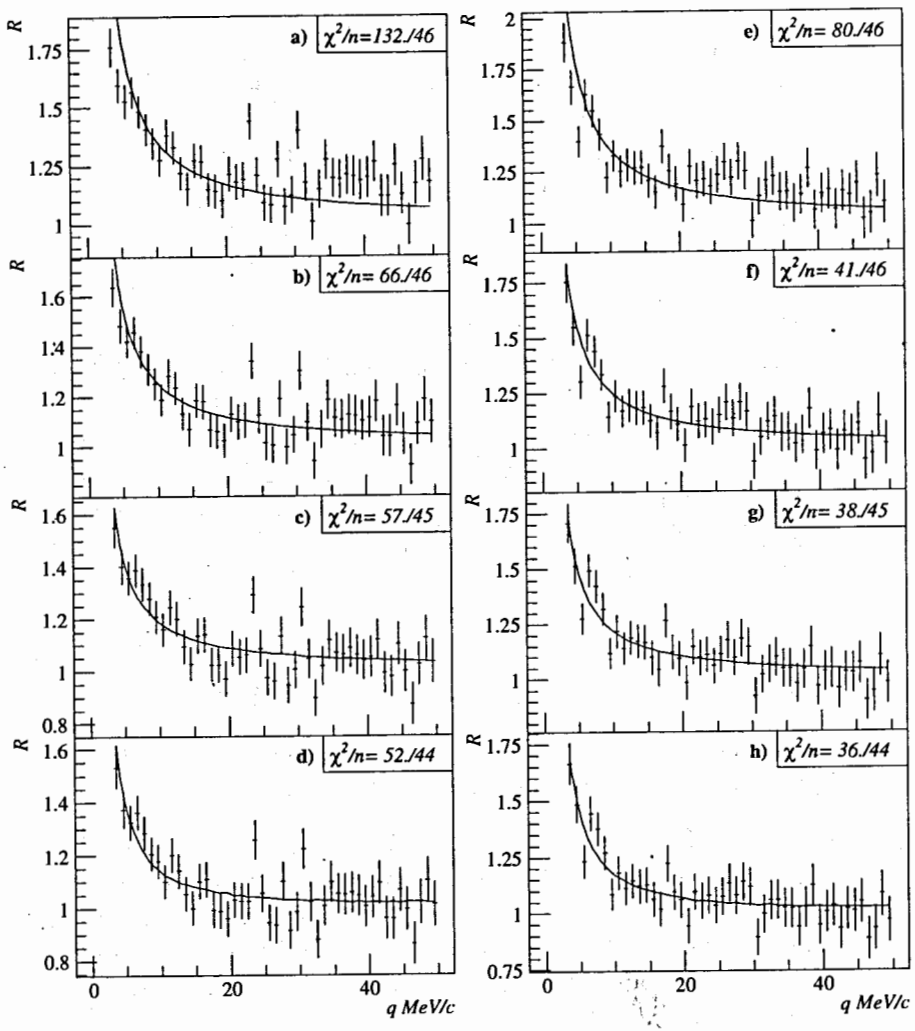

Figure 7: The correlation function versus relative momentum q obtained with "thick" (a–d) and "thin" (e–h) targets fitted by four different modelled functions (solid curves).

Figure 8 shows the distributions of the $\pi^+\pi^-$ pairs over relative momentum in the region $0 < q < 50$ MeV/c for the "thick" (Figs. 8a and 8b) and "thin" (Figs. 8c and 8d) targets. The curves are the three-parameter modelled functions with the parameters determined in the region $q > 3$ MeV/c. As indicated in Fig. 8, an excess of the experimental distribution above the modelled distribution is observed, sizable for the "thick" target and moderate for the "thin" target. The "atomic" pairs account for this excess [20]. The difference in N_A obtained with the "thick" and "thin" targets is explained by different $P_{\rm br}$ values in Eq.(11) for two target thicknesses.

The number of the "atomic" pairs N_A, the expected value of N_A^f and the errors in their difference $\sigma_{\Delta N}$ for two thicknesses of the targets S_t are presented in Table 3. From the cited data it follows that the experimental and expected numbers of the "atomic" pairs are in agreement within the statistical error limits both for the "thick" and the "thin" targets. This allows the conclusion about the adequate description of the $\pi^+\pi^-$ pair distribution considerating the Coulomb interaction in the final state.

Table 3:

S_t μm	N_A	N_A^f	$\sigma_{\Delta N}$
8.0	352. ± 74.	209. ± 16.	89.
1.4	54. ± 65.	43. ± 3.6	68.

6. Yield of pairs from short-lived and long-lived sources

The contribution of the pairs from long-lived sources determined by fitting the distributions in the eight momentum intervals for the "thick" ($l_{\rm tk}$) and "thin" ($l_{\rm tn}$) targets as well as the values of l_L predicted with the Lund model are presented in Table 4.

As follows from the above data the experimentally determined contribution of pairs from long-lived sources is measured with an accuracy of 10% and corresponds to the Lund model calculated values within the statistical error limits except the interval $1675 < p < 1850$ MeV/c for "thick"

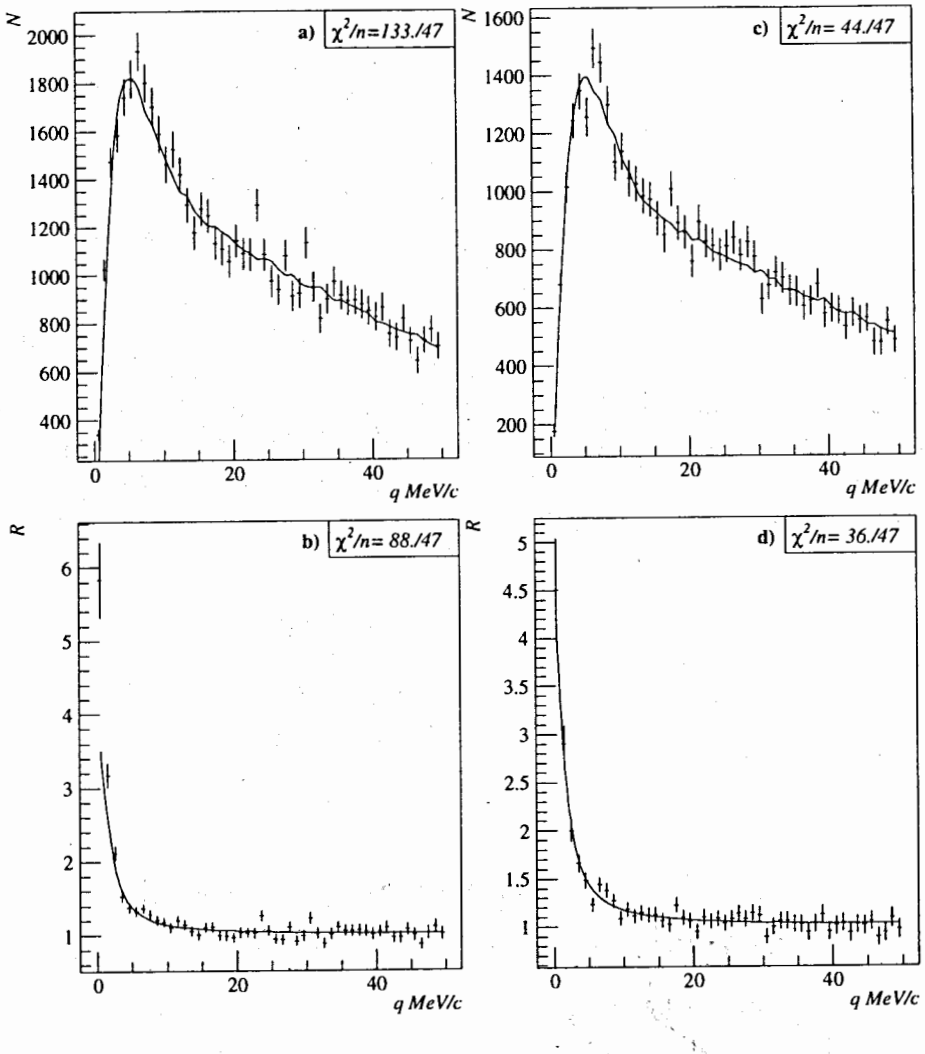

Figure 8: Event distributions over relative momentum q in the interval $0 < q < 50$ MeV/c obtained with the "thick" (a) and "thin" (c) targets. The same distributions are also presented in the form of correlation functions: (b) and (d), respectively.

Table 4:

$p_{\min}$ MeV/c	$p_{\max}$ MeV/c	l_{tk} %	l_{tn} %	l_L %
800.	975.	17.5 ± 9.2	$43. \pm 15.$	47.8
975.	1150.	41.3 ± 7.8	33.7 ± 9.8	43.1
1150.	1325.	35.6 ± 7.4	37.0 ± 9.3	37.9
1325.	1500.	35.2 ± 7.5	31.1 ± 8.8	33.1
1500.	1675.	35.0 ± 8.4	37.8 ± 9.2	28.8
1675.	1850.	$63. \pm 11.$	$32. \pm 11.$	25.0
1850.	2025.	$34. \pm 18.$	$17. \pm 18.$	21.8
2025.	2200.	$47. \pm 49.$	$50. \pm 52.$	19.2
800.	2200.	40.3 ± 4.4	33.2 ± 5.0	31.3

target. But in the same interval for the "thin" target this difference is absent though the ratio of pairs from different sources does not depend on the target thickness. This allows the difference to be considered as a statistical fluctuation.

Thus the effect of Coulomb interaction in the final state allows one to separate pairs in respect to their production region size. This method is suitable for high multiplicity processes.

7. Test of the result stability

We have tested the influence of uncertainties in the setup resolution and admixture of e^+e^- and π^-p pairs on the results.

The setup resolution affects the shape of the "atomic" and "free" pair distributions. To infer how the resolution of the setup in p and $\theta_{1,2}$ affects the "atomic" pair number the values of σ_{q_L} and σ_{q_T} determined in this experiment (see Section 2) were altered independently and jointly by $\pm 10\%$ (σ'_{q_L} and σ'_{q_T}). The results are listed in Table 5. It is shown that a 10% simultaneous resolution variation in q_L and q_T leads to a 7.5% change in N_A for the "thick" target. The accuracy of the difference of N_A for different resolution practically does not include statistical errors of N_A because for all cases the same statistics was used. Consequently, in the calculation of the difference the statistical errors are canceled and the variation of N_A is explained only by the use of different resolution values.

Table 5:

$\frac{\sigma'_{qL}}{\sigma_{qL}}$	$\frac{\sigma'_{qT}}{\sigma_{qT}}$	"thick" target N_A	"thin" target N_A
0.9	1.0	335. ± 75.	35. ± 66.
1.0	1.0	354. ± 74.	55. ± 65.
1.1	1.0	373. ± 73.	74. ± 63.
1.0	0.9	346. ± 75.	55. ± 65.
1.0	1.0	354. ± 74.	55. ± 65.
1.0	1.1	360. ± 74.	56. ± 65.
0.9	0.9	327. ± 76.	35. ± 66.
1.0	1.0	354. ± 74.	55. ± 65.
1.1	1.1	380. ± 73.	75. ± 63.

For the "thin" target the absolute value of the change matches the change for the "thick" target, but the relative change of N_A is substantially greater. This is due to the value of the change being determined by the error in the prediction of the "Coulomb" pair number in the region $q <$ 2 MeV/c and, consequently, by the "Coulomb" pair number itself. The errors in the "Coulomb" pair number for the "thick" and the "thin" target are similar but the number of "atomic" pairs with the "thin" target is much smaller. Therefore the relative error is found to be larger.

The influence of the e^+e^- pair admixture in the distribution dN_t/dq on the number of the "atomic" pairs was tested by adding to this distribution 1%, 2% and 4% admixture of e^+e^- pairs relative to the total number of analyzed events. (The measured value of this admixture was 0.6 %). These pairs were mainly generated in the Dalitz decay $\pi^0 \to e^+ e^- \gamma$ and were recorded for calibrations. The above numbers of e^+e^- pairs were processed as π mesons and added to the distributions of the $\pi^+\pi^-$ pairs. In Table 6 the corresponding changes of N_A are presented. It is seen that the real admixture (0.6%) of e^+e^- pairs does not affect the final results.

A change of N_A was also obtained supposing that there has been incorrect subtraction of π^-p and πK admixtures from the accidental event distribution. To test the scale of N_A variation this value was calculated without the correction of the detected spectra for the contribution of protons and K mesons by replacing the distribution $\Phi(q)$ by dN_a/dq (see Section 4). It leads to:

$$N_A^{\rm tk} = 356 \pm 75\ , \quad N_A^{\rm tn} = 50 \pm 64\ . \tag{22}$$

The differences between these values and N_A given in Table 3 are negligible.

Table 6:

$n_{\rm el}$ %	"thick" target N_A	"thin" target N_A
0.	352. ± 74.	54. ± 65.
1.	354. ± 74.	56. ± 65.
2.	354. ± 75.	57. ± 65.
4.	350. ± 76.	51. ± 65.

8. Conclusions

In the present experiment the correlation function of the $\pi^+\pi^-$ pairs in the region of the Coulomb interaction in the final state was measured. The ratio of pairs from the short-lived and long-lived sources was determined. The $\pi^+\pi^-$ pairs with the relative momentum $q <$ 2 MeV/c onto the "atomic", "Coulomb" and "non-Coulomb" pairs were separated, which allowed observation of $\pi^+\pi^-$ atoms [20] and estimation of their lifetime [21].

The possibility of using the Coulomb effect to separate charged particle pairs according to the size of the particle production region was demonstrated.

The measurement of the $\pi^+\pi^-$ correlation function provides the experimental ground for the "Coulomb" corrections used in the experiments for the Bose-Einstein correlation [9].

References

[1] *Sakharov A.D.//* Zh. Eksp. Teor. Fiz., 1948, V.18, P.631.

[2] *Afanasyev L.G et al.//* Phys. Lett. B, 1991, V.255, P.146.

[3] *Wiencke L.K. et al//* Phys. Rev. D, 1992, V.46, P.3708.

[4] *Harris J. and Brown L.M.//* Phys. Rev., 1957, V.105, P.1656.

[5] *Erazmus B. et al.//* Phys. Rev. C, 1994, V.49, P.349.

[6] *Bayer V.N. and Fadin V.S.//* Zh. Eksp. Teor. Fiz., 1969, V.57, P.225 .

[7] *Arbuzov A.B.//* Nuovo Cimento, 1994, V.107A, P.1263.

[8] *Li B.A//* Phys. Lett., 1995, V.B346, P.5.

[9] *Biyajima M. et al.//* Phys. Lett., 1995, V.B353, P.340.

[10] *Kopylov G.E. and Podgoretsky M.I.//* Yad. Fiz., 1972, V.15, P.392.

[11] *Ford W.T. et al.//* Phys. Lett., 1972, V.B38, P.335.

[12] *Lepage G.P.//* Phys. Rev. D, 1990, V.42, P.3251.

[13] *Fadin V.S. et al.//* Phys. Rev. D, 1995, V.52, P.1377.

[14] *Nemenov L.L.//* Yad. Fiz., 1985, V.41, P.980.

[15] *Afanasyev L.G. et al.//* Yad. Fiz., 52, V.1990, P.1046.

[16] *Uretsky J. and Palfrey J.//* Phys. Rev., 1961, V.121, P.1798.

[17] *Bilenky S.M. et al//* Yad. Fiz., 1969, V.10, P.812.

[18] *Gasser J. and Leutwyler H.//* Ann. Phys., 1984, V.158, P.142.

[19] *Afanasyev L.G. and Tarasov A.V.//* Preprint JINR E4-95-344, Dubna, 1995, to appear in Yad.Fiz.

[20] *Afanasyev L.G. et al.//* Phys. Lett., 1993, V.B308, P.200.

[21] *Afanasyev L.G. et al.//* Phys. Lett. B, 1994, V.338, P.478.

[22] *Adeva B. et al.//* Lifetime measurement of $\pi^+\pi^-$ atoms to test low energy QCD predictions., Proposal to the SPS LC, CERN/SPSLC 95-1, SPSLC/P 284, Geneva 1995

[23] *Uribe J. et al.//* Phys. Rev. D, 1994, V.49, P.4373.

[24] *Lednitski R. and Ljuboschitz V.L.//* Yad. Fiz., 1982, V.35, P.1316.

[25] *Lednitski R. and Ljuboschitz V.L.//* Proc. Int. Workshop on Particle Correlations and Interferometry in Nuclear Collisions, CORINE90, Nantes, June 28-30, 1990, p.42.

Received by Publishing Department
on July 10, 1996.

Афанасьев Л.Г. и др. E1-96-256

Измерение эффекта кулоновского взаимодействия в $\pi^+\pi^-$-парах из реакции $p\mathrm{Ta} \to \pi^+\pi^- X$ при энергии 70 ГэВ

Исследовалось рождение $\pi^+\pi^-$-пар в реакции $p\mathrm{Ta} \to \pi^+\pi^- X$ при энергии 70 ГэВ. Измерена двухчастичная корреляционная функция в интервале относительных импульсов в с.ц.м. пары $0 \le q \le 50$ МэВ/с при импульсах пионов в лабораторной системе от 0,8 до 2,4 ГэВ/с. Кулоновское взаимодействие π-мезонов в конечном состоянии резко увеличивает выход $\pi^+\pi^-$-пар с $q < 10$ МэВ/с для пионов, образованных в области размером много меньше $1/m_\pi\alpha$. Эффект кулоновского взаимодействия позволил разделить $\pi^+\pi^-$-пары в зависимости от размера области генерации.

Работа выполнена в Лаборатории ядерных проблем ОИЯИ.

Препринт Объединенного института ядерных исследований. Дубна, 1996

Afanasyev L.G. et al. E1-96-256

Measurement of the Coulomb Interaction Effect in $\pi^+\pi^-$ Pairs from the Reaction $p\mathrm{Ta} \to \pi^+\pi^- X$ at 70 GeV

Production of $\pi^+\pi^-$ pairs was studied for the reaction $p\mathrm{Ta} \to \pi^+\pi^- X$ at 70 GeV. For the pions with lab momenta from 0.8 to 2.4 GeV/c the two-particle correlation function was measured in the interval of the c.m.s. relative momentum $0 \le q \le 50$ MeV/c. The Coulomb final state interaction for pions produced in a region much smaller than $1/m_\pi\alpha$ leads to a sharp increase in the yield of $\pi^+\pi^-$ pairs with $q < 10$ MeV/c. The effect of the Coulomb interaction has allowed separation of the $\pi^+\pi^-$ pairs with respect to the size of their production region.

The investigation has been performed at the Laboratory of Nuclear Physics, JINR.

Preprint of the Joint Institute for Nuclear Research. Dubna, 1996